

Engineering Organic Sensitizers for Iodine-Free Dye-Sensitized Solar Cells: Red-Shifted Current Response Concomitant with Attenuated Charge Recombination

Yu Bai,^{†,‡} Jing Zhang,[†] Difei Zhou,^{†,‡} Yinghui Wang,[†] Min Zhang,[†] and Peng Wang^{*,†}

[†]State Key Laboratory of Polymer Physics and Chemistry, Changchun Institute of Applied Chemistry, Chinese Academy of Sciences, Changchun 130022, China

[‡]Graduate School, Chinese Academy of Sciences, Beijing 10039, China

S Supporting Information

ABSTRACT: With a new metal-free donor–acceptor photosensitizer featuring the 2,6-bis(thiophen-2-yl)-4,4-dihexyl-4*H*-cyclopenta[2,1-*b*:3,4-*b'*]dithiophene-conjugated spacer and the tris(1,10-phenanthroline)cobalt(II/III) redox shuttle, we present a highly efficient iodine-free dye-sensitized solar cell displaying a power conversion efficiency of 9.4% measured at 100 mW cm^{−2} simulated AM1.5 conditions.

Dye-sensitized solar cells (DSCs) are presently under intense academic and industrial investigations because of their grand potential to serve as a low-cost alternative to existing photovoltaic technologies.¹ A state-of-the-art DSC fabricated by sensibly combining a panchromatic ruthenium dye,² an iodine electrolyte, and a thick mesoporous titania film has been notarized with a record solar-to-electricity conversion efficiency of 11.1% thus far.³ Owing to a resource restriction of the noble metal ruthenium, metal-free organic push–pull dyes have been actively pursued for the wide availability of their raw materials.⁴ In this context, impressive progress on iodine-free DSCs displaying an excellent photovoltage has been attained very recently, based upon the combination of high-absorptivity organic dyes with either a solid organic hole-transporter⁵ or some iron-,⁶ cobalt-,⁷ and copper-containing⁸ redox shuttles, all of which feature considerably downward-shifted Fermi levels with respect to the common iodine electrolytes. However, these explorations have not yet afforded power conversion efficiencies comparable to those of champion DSCs based on organic dyes and iodine electrolytes.^{4d–f} In this work, we employ 2,6-bis(thiophen-2-yl)-4,4-dihexyl-4*H*-cyclopenta[2,1-*b*:3,4-*b'*]dithiophene as the π -conjugated linker to synthesize a new dye, coded C229 (Figure 1A), which exhibits outstanding efficiencies of 9.4–10.3% in DSCs based on the tris(1,10-phenanthroline)cobalt electrolyte.

In comparison with the C228 dye (Figure 1A) possessing the 2,7-bis(thiophen-2-yl)-9,9-dihexylfluorene segment, C229 takes on an augmented maximum molar absorption coefficient at a desirable longer wavelength (as shown in Supporting Information (SI), Figure S1), owing to a better electron delocalizability of its π -conjugated spacer.⁹ We further examined the photocurrent action spectra (Figure 1B) of DSCs with C228 or C229 dye, in conjunction with an iodine-free electrolyte composed of 0.3 M tris(1,10-phenanthroline)cobalt(II)

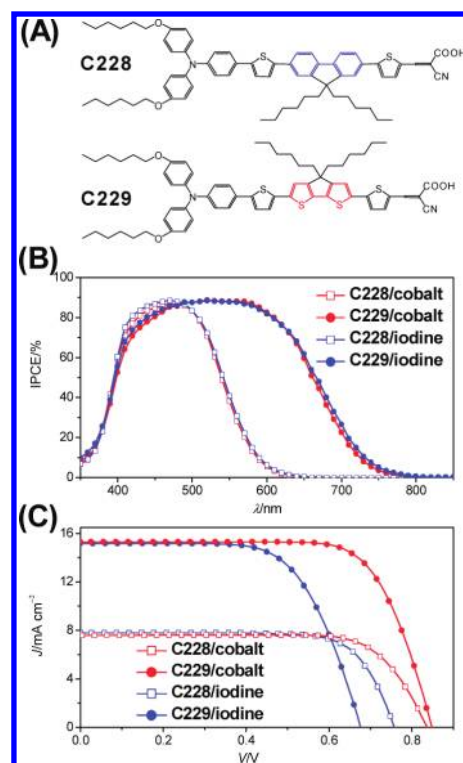


Figure 1. (A) Dye structures. (B) Photocurrent action spectra of C228 and C229 cells employing an iodine or cobalt electrolyte. (C) J – V characteristics measured at 100 mW cm^{−2} simulated AM1.5 conditions. A (2.7+4.1)- μ m-thick bilayer titania film was employed for cell fabrication. An antireflection film was adhered to a testing cell during measurement. All cells were measured with a metal mask having an aperture area of 0.158 cm². The spectral distribution of our light resource simulates the AM1.5 solar emission (ASTM G173-03). The validity of our data is further confirmed by comparing the overlap integral of the measured IPCE spectrum with the standard AM1.5 solar emission spectrum and the experimental J_{sc} showing <5% error.

di[bis(trifluoromethanesulfonyl)imide] (Co-phen), 75 mM nitrosonium tetrafluoroborate (NOBF₄), 0.1 M lithium bis(trifluoromethanesulfonyl)imide (LiTFSI), and 0.5 M 4-*tert*-butylpyridine (TBP) in acetonitrile. Apart from a comparable

Received: April 22, 2011

Published: July 07, 2011

Table 1. Photovoltaic Parameters^a

| electrolyte ^b | <i>d</i> /μm | <i>P</i> _{in} /mW cm ⁻² | <i>J</i> _{sc} /mA cm ⁻² | <i>V</i> _{oc} /V | FF | η/% |
|--------------------------|--------------|---|---|---------------------------|------|------|
| C228 Dye | | | | | | |
| cobalt | 2.7 + 4.1 | 100.00 | 7.60 | 0.83 | 0.74 | 4.7 |
| iodine | 2.7 + 4.1 | 100.00 | 7.78 | 0.76 | 0.74 | 4.4 |
| C229 Dye | | | | | | |
| cobalt | 2.7 + 4.1 | 12.48 | 1.92 | 0.77 | 0.79 | 9.3 |
| | | 23.27 | 3.58 | 0.79 | 0.78 | 9.6 |
| | | 50.09 | 7.74 | 0.82 | 0.76 | 9.7 |
| | | 100.00 | 15.31 | 0.85 | 0.73 | 9.4 |
| | 5.0 + 4.1 | 12.48 | 2.08 | 0.76 | 0.80 | 10.2 |
| | | 23.27 | 3.88 | 0.79 | 0.78 | 10.3 |
| | | 50.09 | 8.32 | 0.82 | 0.74 | 10.1 |
| iodine | 2.7 + 4.1 | 100.00 | 15.20 | 0.84 | 0.70 | 8.4 |
| | | 100.00 | 15.20 | 0.68 | 0.65 | 6.7 |

^a The spectral distribution of our light resource simulates the AM1.5 solar emission (ASTM G173-03) with a mismatch of <5%. *d*, thickness of titania film; *P*_{in}, incident light intensity. ^b Cobalt electrolyte: 0.3 M Co-phen, 75 mM NOBF₄, 0.1 M LiTFSI, and 0.5 M TBP in acetonitrile. Iodine electrolyte: 0.3 M DMII, 75 mM I₂, 0.1 M LiTFSI, and 0.5 M TBP in acetonitrile.

summit of incident photon-to-collected electron conversion efficiencies (IPCEs) of ~88%, the photosensitizer transformation from C228 to C229 brings on ~150 nm red-shifting of the photocurrent onset wavelength.

The solar-to-electricity conversion efficiencies of these two cobalt cells were also evaluated by recording the *J*–*V* characteristics at 100 mW cm⁻² simulated AM1.5 conditions, and the detailed photovoltaic parameters are collected in Table 1. As Figure 1C presents, the short-circuit photocurrent density (*J*_{sc}), open-circuit photovoltage (*V*_{oc}), and fill factor (FF) of the C228 cell are 7.6 mA cm⁻², 0.83 V, and 0.74, respectively, generating a power conversion efficiency (η) of 4.7%. In good accord with the integrals of IPCEs over the standard AM1.5 solar emission spectrum, the C229 dye evokes a notably improved *J*_{sc} = 15.31 mA cm⁻², which affords a 2 times higher η = 9.4%, with an impressive *V*_{oc} = 0.85 V. Three batches of 12 cells exhibit an efficiency ranging from 9.3% to 9.6% (see SI, including Figure S2 and Table S1, for details). Note that other organic sensitizers previously reported by our group all present lower efficiencies in cells employing iodine-free electrolytes. The new record efficiency of 9.4% achieved in full sunlight constitutes a breakthrough, setting a new benchmark for iodine-free DSCs.⁷ With a thicker bilayer titania film, impressive power conversion efficiencies of >10% (Table 1) under relatively weak light irradiation have been achieved with C229.

To clarify the importance of combining iodine-free redox couples with organic dyes, an iodine control electrolyte consisting of 0.3 M 1,3-dimethylimidazolium iodide (DMII), 75 mM iodine, 0.5 M TBP, and 0.1 M LiTFSI in acetonitrile was further formulated to fabricate the iodine control cells. As Figure 1B depicts, the dye substitution of C228 with C229 affects the photocurrent action spectra of the iodine cells in a similar pattern as the cobalt counterparts. *J*–*V* characteristics of these iodine cells measured under full sunlight are also included in Figure 1C for comparison, with the detailed photovoltaic parameters listed in Table 1. It is noted that, regardless of the electrolyte selection, the C229 dye displays a better cell efficiency, proving the

Table 2. Parameters^a Derived From Electrical Impedance Analyses

| dye/electrolyte | <i>E</i> _c – <i>E</i> _{F,redox} /eV | <i>n</i> _c /10 ¹⁶ cm ⁻³ | <i>U</i> _{0k} /10 ²⁰ cm ⁻³ s ⁻¹ |
|-----------------|---|--|---|
| C228/cobalt | 1.05 ± 0.003 | 13 ± 3 | 320 ± 30 |
| C229/cobalt | 1.02 ± 0.004 | 92 ± 8 | 34 ± 4 |
| C228/iodine | 0.96 ± 0.002 | 28 ± 5 | 9 ± 2 |
| C229/iodine | 0.93 ± 0.003 | 4 ± 1 | 2800 ± 90 |

^a *E*_c, titania conduction band edge; *E*_{F,redox}, electrolyte Fermi-level; *n*_c, free electron density of our cells at the 100 mW cm⁻² AM1.5 conditions; *U*_{0k}, effective rate constant of charge recombination at the titania/electrolyte interface. The errors are estimated from measurements on three cells.

superiority of employing cyclopentadithiophene relative to fluorine as the conjugated spacer in D–π–A dyes. This concept is actually borrowed from the wonderful design of a historically seminal conjugated D–A polymer.¹⁰ Note that, in our earlier work,¹¹ we proved the advantage of cyclopentadithiophene relative to dithiophene in the DSC dye design, and this strategy was also applied by Grätzel's group.^{7d} In contrast to the cobalt cells, the iodine congeners exhibit evidently attenuated *V*_{oc}, which can be primarily ascribed to a 0.23 V negative shift of the electrolyte equilibrium potential (SI, Figure S3; iodine, –0.30 V and cobalt, –0.07 V versus Fc⁺/Fc). Moreover, it is noteworthy that the dye alteration in the iodine cells from C228 to C229 has caused a *V*_{oc} attenuation of 0.08 V, sharply contrasting a 0.02 V enhancement in the cobalt cells.

The open-circuit photovoltage of a DSC under illumination is regarded as the energy difference between the Fermi level of titania (*E*_{F,n}) and that of a redox electrolyte (*E*_{F,redox}), as described by *V*_{oc} = (*E*_{F,n} – *E*_{F,redox})/*e*, where *e* is the elementary charge. The opposite *V*_{oc} variation for the cobalt and iodine cells in the case of sensitizer change from C228 to C229 must stem from a redox-couple-correlated alternation of *E*_{F,n} level, which could be understood via *E*_{F,n} = *E*_c + *k*_B*T* ln(*n*_c/*N*_c). Here, *E*_c is the titania conduction band edge, *k*_B the Boltzmann constant, *T* the absolute temperature, *n*_c the free carrier density, and *N*_c the density of accessible states in the conduction band. The quantity of *E*_c – *E*_{F,redox} could be roughly estimated by analyzing the chemical capacitance (*C*_μ) of titania films¹² (see SI for details). Numerical analysis of an electrical impedance spectroscopy using the transmission line model¹³ can afford the *C*_μ at a given potential bias (*V*). Fitting the *C*_μ data in Supporting Information Figure S4A yields the *E*_c – *E*_{F,redox} values, and the results are collected in Table 2. Apparently, a downward *E*_c shift of 30 meV arises in both electrolytes upon replacing C228 with C229.

On the basis of this analysis, we can estimate *n*_c (Table 2) of each cell at open circuit under full sunlight via *n*_c = *N*_c exp{[*eV*_{oc} – (*E*_c – *E*_{F,redox})]/*k*_B*T*} (see SI for details). It is noticed from Table 2 that, upon employing the cobalt electrolyte, the C229 cell contains more charges than the C228 counterpart, which could be ascribed to better light absorption and slow charge recombination in the case of C229; however, the use of the iodine electrolyte evokes an even lower *n*_c level in the C229 cell than in the C228 congener. The validity of this deduction could be further elaborated by comparing the effective charge recombination rate constant, *U*_{0k}, which can be obtained by analyzing interfacial charge recombination resistances *R*_{ct} (SI, Figure S4B).¹⁴ In the cobalt cells, C229 prompts a *U*_{0k} almost 1 order of magnitude smaller than that with C228 (Table 2).

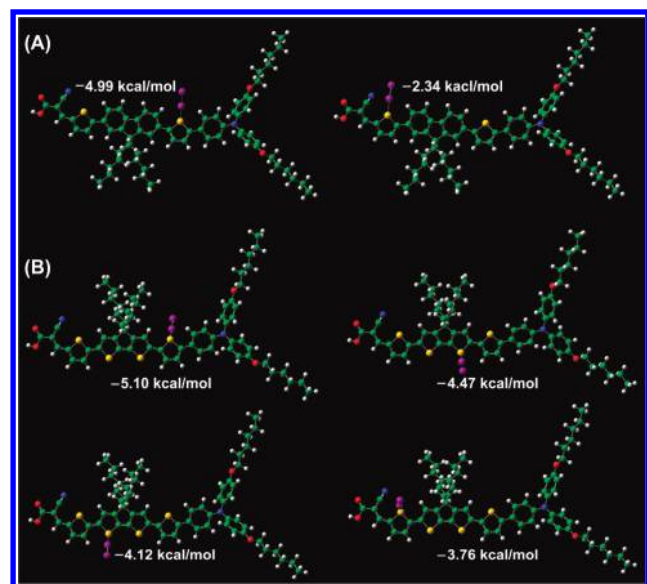


Figure 2. Optimized geometries of (A) C228–I₂ and (B) C229–I₂ complexes. The interaction energies between iodine and sulfur atoms are also included. Iodine, purple; carbon, green; sulfur, yellow; nitrogen, blue; oxygen, red; hydrogen, gray.

Upon replacing the cobalt electrolyte with the iodine one, however, a >2 orders of magnitude larger U_{0k} , i.e., faster charge recombination, is observed for the C229 cell relative to the C228 counterpart (C228, $9 \times 10^{20} \text{ cm}^{-3} \text{ s}^{-1}$; C229, $2800 \times 10^{20} \text{ cm}^{-3} \text{ s}^{-1}$). These comparisons, coupled with the preceding discussion on $E_c - E_{F, \text{redox}}$ provide sound evidence for the aforementioned redox-couple-related V_{oc} variation from C228 to C229.

To gain insight into the redox-shuttle-correlated interfacial charge recombination kinetics, we further resorted to quantum calculation to evaluate the interaction between dye molecules and electron acceptors in electrolytes, which may affect the distribution profile of oxidized species near the titania nanocrystal surface. It is known that electron-deficient halogen atoms such as iodine can form complexes with other electron-rich atoms through a non-covalent interaction, i.e., halogen bonding.¹⁵ The adverse impact of possible halogen bonding on interfacial charge recombination in DSCs has been proposed by several groups,¹⁶ but no very convincing spectral data have been reported so far. The redox-couple-correlated variation of charge recombination upon dye alternation presented in this paper has supplied a new clue to understand the halogen-bonding issue in DSCs. Herein we compare the interaction energies of dye–I₂ complexes for C228 and C229. Our calculation results (Figure 2) show that, with respect to C228, the C229 dye contains more interaction sites (sulfur atoms), favoring the formation of dye–I₂ complexes. Thereby, we may expect a much higher iodine concentration in the vicinity of a C229 dye-coated titania interface, leading to accelerated interfacial charge recombination.

Although the variation of redox shuttle from iodine to cobalt does not exert a noticeable influence on the IPCE summit of DSCs based on the C228 or C229 dye, it is still valuable to measure the dual-channel charge-transfer kinetics of oxidized dye molecules with titania electrons and electron-donating species in electrolytes.¹⁷ We first recorded the transient absorption spectrum (Figure 3A) of a C228 or C229 dye-coated titania film with an intensified charge-coupled detector camera. It can be noticed

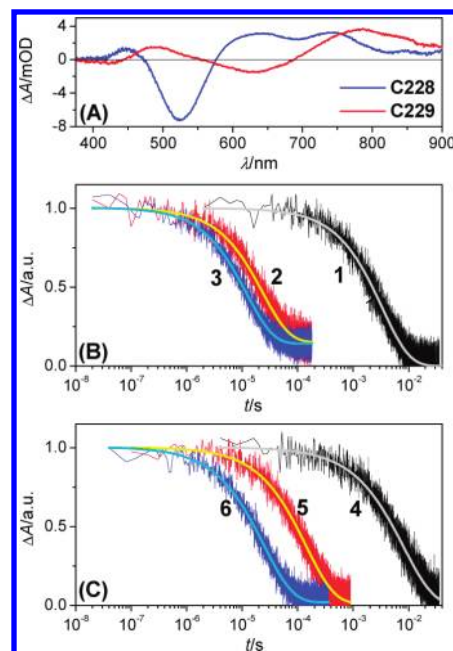


Figure 3. (A) Transient absorption spectra of 2.4- μm -thick dye-coated titania films immersed in an inert electrolyte of 0.1 M LiTFSI and 0.5 M TBP in acetonitrile. The spectra were recorded upon nanosecond laser excitation at 500 nm. (B) Absorption decays of $\sim 11\text{-}\mu\text{m}$ -thick C228-coated titania film in the inert (1), iodine (2), and cobalt (3) electrolytes. The compositions of our iodine and cobalt electrolytes are described in the text. Excitation wavelength and pulse fluence: $45 \mu\text{J cm}^{-2}$ at 552 (trace 1), 555 (trace 2), and 551 nm (trace 3). Probe wavelength, 782 nm. (C) Absorption decays of $\sim 11\text{-}\mu\text{m}$ -thick, C229-coated titania films immersed in the inert (4), iodine (5), and cobalt (6) electrolytes. Excitation wavelength and pulse fluence, $36 \mu\text{J cm}^{-2}$ at 683 (trace 4), 687 (trace 5), and 682 nm (trace 6); probe wavelength, 782 nm. The smooth lines in panels B and C are stretched exponential fittings over raw data obtained by averaging over 500 laser shots.

that, with respect to their neutral counterparts, both oxidized C228 and C229 dye molecules display strong absorption in the near-infrared region. Because of the signal sensitivity of our photomultiplier tube detector, a 782-nm probe light and a thick titania film were used in the following kinetic measurements. The excitation wavelengths were also carefully selected according to an optical density of ~ 0.2 of dye-coated titania films, ensuring a similar electron distribution profile in the studied samples. In the presence of an inert electrolyte, the slow absorption decays (traces 1 and 4 in Figure 3B,C) can be attributed to the back electron transfer from titania to oxidized dye molecules. Furthermore, obviously accelerated absorption decays (traces 2, 3, 5, and 6) were observed upon using the practical cobalt or iodine electrolyte, owing to the occurrence of dye regeneration by either cobalt(II) or iodide ions. The average time ($\langle \tau \rangle$) of these charge-transfer processes was derived by fitting the traces to a stretched exponential function ($\Delta A \propto A \exp(-(t/\tau)^\alpha)$, collected in SI Table S2). The kinetic branch ratios of oxidized dye molecules involving dual-channel charge-transfer reactions exceed 50 in all our cells, ensuring an efficient interfacial charge separation. A ~ 50 mV negative movement of the formal redox potential from C228 to C229 (SI, Figure S5) induces a general deceleration of dye regeneration in both cobalt and iodine electrolytes, which however exhibit a distinctive variation for the two redox couples (iodine, ~ 7 -fold deceleration; cobalt, ~ 2 -fold

deceleration). This valuable observation suggests that, in comparison with the canonical iodine electrolyte, the cobalt counterpart should endow a large chance of uplifting the ground-state redox potential in the further design of low energy gap push–pull dyes to harvest near-infrared solar photons.

To summarize, we have demonstrated an iodine-free dye-sensitized solar cell exhibiting an unprecedented power conversion efficiency of 9.4% at 100 mW cm^{−2} simulated AM1.5G conditions, based on a new organic push–pull dye C229 in conjunction with the tris(1,10-phenanthroline)cobalt(II/III) redox shuttle. With respect to its C228 counterpart, the C229 dye, when combined with the cobalt electrolyte, not only evokes a red-shifted photocurrent response but concomitantly prompts a *V*_{oc} improvement, in sharp contrast to a *V*_{oc} decrease for the iodine control cells. This is further rationalized in terms of the redox-couple-correlated dependence of dye structures on charge recombination kinetics at the titania/electrolyte interface via a joint electrical impedance and quantum calculation analysis. Our work will shed light on further exploration of near-infrared-absorption organic photosensitizers for more efficient iodine-free mesoscopic titania solar cells.

■ ASSOCIATED CONTENT

S **Supporting Information.** Experimental details, impedance data analysis, and additional experimental data. This material is available free of charge via the Internet at <http://pubs.acs.org>.

■ AUTHOR INFORMATION

Corresponding Author
peng.wang@ciac.jl.cn

■ ACKNOWLEDGMENT

The National 973 Program (No. 2007CB936702 and No. 2011CBA00702), the National Science Foundation of China (No. 50973105), the CAS Knowledge Innovation Program (No. KG CX2-YW-326), and the CAS Hundred Talent Program are acknowledged for financial support. We are grateful to Dyesol for supplying the scattering paste and to DuPont Packaging and Industrial Polymers for supplying the Bynel film.

■ REFERENCES

- (1) Grätzel, M. *Acc. Chem. Res.* **2009**, *42*, 1788.
- (2) Nazeeruddin, M. K.; Péchy, P.; Renouard, T.; Zakeeruddin, S. M.; Humphry-Baker, R.; Comte, P.; Liska, P.; Cevey, L.; Costa, E.; Shklover, V.; Spiccia, L.; Deacon, G. B.; Bignozzi, C. A.; Grätzel, M. *J. Am. Chem. Soc.* **2001**, *123*, 1613.
- (3) Chiba, Y.; Islam, A.; Watanabe, Y.; Komiya, R.; Koide, N.; Han, L. *Jpn. J. Appl. Phys.* **2006**, *45*, L638.
- (4) For example, see: (a) Horiuchi, T.; Miura, H.; Sumioka, K.; Uchida, S. *J. Am. Chem. Soc.* **2004**, *126*, 12218. (b) Kim, S.; Lee, J. K.; Kang, S. O.; Ko, J.; Yum, J.-H.; Fantacci, S.; De Angelis, F.; Di Censo, D.; Nazeeruddin, M. K.; Grätzel, M. *J. Am. Chem. Soc.* **2006**, *128*, 16701. (c) Koumura, N.; Wang, Z. S.; Mori, S.; Miyashita, M.; Suzuki, E.; Hara, K. *J. Am. Chem. Soc.* **2006**, *128*, 14256. (d) Ito, S.; Miura, H.; Uchida, S.; Takata, M.; Sumioka, K.; Liska, P.; Comte, P.; Péchy, P.; Grätzel, M. *Chem. Commun.* **2008**, 5194. (e) Zeng, W.; Cao, Y.; Bai, Y.; Wang, Y.; Shi, Y.; Zhang, M.; Wang, F.; Pan, C.; Wang, P. *Chem. Mater.* **2010**, *22*, 1915. (f) Choi, H.; Raabe, I.; Kim, D.; Teocoli, F.; Kim, C.; Song, K.;

Yum, J.-H.; Ko, J.; Nazeeruddin, M. K.; Grätzel, M. *Chem.—Eur. J.* **2010**, *16*, 1193.

(5) Cai, N.; Moon, S.-J.; Cevey-Ha, L.; Moehl, T.; Humphry-Baker, R.; Wang, P.; Zakeeruddin, S. M.; Grätzel, M. *Nano Lett.* **2011**, *11*, 1452.

(6) Daenke, T.; Kwon, T.-H.; Holmes, A. B.; Duffy, N. W.; Bach, U.; Spiccia, L. *Nat. Chem.* **2011**, *3*, 211.

(7) (a) Feldt, S. M.; Gibson, E. A.; Gabrielsson, E.; Sun, L.; Boschloo, G.; Hagfeldt, A. *J. Am. Chem. Soc.* **2010**, *132*, 16714. (b) Zhou, D.; Yu, Q.; Cai, N.; Bai, Y.; Wang, Y.; Wang, P. *Energy Environ. Sci.* **2011**, *4*, 2030. (c) Zhang, M.; Liu, J.; Wang, Y.; Zhou, D.; Wang, P. *Chem. Sci.* **2011**, *2*, 1401. (d) Tsao, H. N.; Yi, C.; Moehl, T.; Yum, J.-H.; Zakeeruddin, S. M.; Nazeeruddin, M. K.; Grätzel, M. *ChemSusChem* **2011**, *4*, 591. (e) Liu, J.; Zhang, J.; Xu, M.; Zhou, D.; Jing, X.; Wang, P. *Energy Environ. Sci.* **2011**, doi: 10.1039/c1ee01633d.

(8) Bai, Y.; Yu, Q.; Cai, N.; Wang, Y.; Zhang, M.; Wang, P. *Chem. Commun.* **2011**, 47, 4376.

(9) Roncali, J. *Macromol. Rapid Commun.* **2007**, *28*, 1761.

(10) (a) Mühlbacher, D.; Scharber, M.; Morana, M.; Zhu, Z.; Waller, D.; Gaudiana, R.; Brabec, C. *Adv. Mater.* **2006**, *18*, 2884. (b) Zhang, M.; Tsao, H. N.; Pisula, W.; Yang, C.; Mishra, A. K.; Müllen, K. *J. Am. Chem. Soc.* **2007**, *129*, 3472.

(11) Li, R.; Liu, J.; Cai, N.; Zhang, M.; Wang, P. *J. Phys. Chem. B* **2010**, *114*, 4461.

(12) (a) Bisquert, J. *Phys. Chem. Chem. Phys.* **2003**, *5*, 5360. (b) Barea, E. M.; Ortiz, J.; Payá, F. J.; Fernández-Lázaro, F.; Fabregat-Santiago, F.; Sastre-Santos, A.; Bisquert, J. *Energy Environ. Sci.* **2010**, *3*, 1985.

(13) Bisquert, J. *J. Phys. Chem. B* **2002**, *106*, 325.

(14) Barea, E. M.; Zafer, C.; Gultekin, B.; Aydin, B.; Koyuncu, S.; Icli, S.; Fabregat-Santiago, F.; Bisquert, J. *J. Phys. Chem. C* **2010**, *114*, 19840.

(15) (a) Metrangolo, P.; Resnati, G. *Chem.—Eur. J.* **2001**, *7*, 2511. (b) Auffinger, P.; Hays, F. A.; Westhof, E.; Ho, P. S. *Proc. Natl. Acad. Sci. U.S.A.* **2004**, *101*, 16789. (c) Nguyen, H. L.; Horton, P. N.; Hursthouse, M. B.; Legon, A. C.; Bruce, D. W. *J. Am. Chem. Soc.* **2004**, *126*, 16. (d) Metrangolo, P.; Neukirch, H.; Pilati, T.; Resnati, G. *Acc. Chem. Res.* **2005**, *38*, 386. (e) Sun, A.; Lauher, J. W.; Goroff, N. S. *Science* **2006**, *312*, 1030. (f) Politzer, P.; Lane, P.; Concha, M. C.; Ma, Y.; Murray, J. S. *J. Mol. Model.* **2007**, *13*, 305. (g) Voth, A. R.; Khuu, P.; Oishi, K.; Ho, P. S. *Nat. Chem.* **2009**, *1*, 74. (h) Legon, A. C. *Phys. Chem. Chem. Phys.* **2010**, *12*, 7736. (i) Metrangolo, P.; Resnati, G. *Nat. Chem.* **2011**, *3*, 260.

(16) (a) O'Regan, B. C.; López-Duarte, I.; Martínez-Díaz, M. V.; Forneli, A.; Albero, J.; Morandeira, A.; Palomares, E.; Torres, T.; Durrant, J. R. *J. Am. Chem. Soc.* **2008**, *130*, 2906. (b) Privalov, T.; Boschloo, G.; Hagfeldt, A.; Svensson, P. H.; Kloo, L. *J. Phys. Chem. C* **2009**, *113*, 783. (c) Planells, M.; Pellejà, L.; Clifford, J. N.; Pastore, M.; De Angelis, F.; López, N.; Marder, S. R.; Palomares, E. *Energy Environ. Sci.* **2011**, *4*, 1820.

(17) (a) O'Regan, B. C.; Durrant, J. R. *Acc. Chem. Res.* **2009**, *42*, 1799. (b) Ardo, S.; Meyer, G. J. *Chem. Soc. Rev.* **2009**, *38*, 115.